

## AFORS Autonomous Fibre-Optic Rotational Seismograph: Design and Application

Leszek R. JAROSZEWICZ<sup>1</sup>, Zbigniew KRAJEWSKI<sup>1</sup>, Henryk KOWALSKI<sup>2</sup>,  
Grzegorz MAZUR<sup>2</sup>, Paweł ZINÓWKO<sup>3</sup>, and Jerzy KOWALSKI<sup>4</sup>

<sup>1</sup>Institute of Applied Physics, Military University of Technology, Warszawa, Poland  
e-mails: jarosz@wat.edu.pl (corresponding author), zkrajewski@wat.edu.pl

<sup>2</sup>Institute of Computer Science, Warsaw University of Technology,  
Warszawa, Poland, e-mails: kowalski@ii.pw.edu.pl, g.mazur@ii.pw.edu.pl

<sup>3</sup>ELPROMA Electronics Ltd, Łomianki, Poland, e-mail: pawel@elproma.com.pl

<sup>4</sup>m-Soft Ltd, Warszawa, Poland, e-mail: jkk@m-soft.pl

### Abstract

We outline the research leading to development of the Autonomous Fibre-Optic Rotational Seismograph (AFORS) and describe the final version of the instrument. The instrument with linear changes of sensitivity keeps accuracy from  $5.1 \times 10^{-9}$  to  $5.5 \times 10^{-8}$  rad/s in the detection bandpass 1.66-212.30 Hz; it is designed for a direct measurement of rotational components emitted during seismic events. The presented system is based on the optical part of the fibre optic gyro construction where a special autonomous signal processing unit (ASPU) optimizes its operation for the measurement of rotation motions instead of the angular changes. The application of a newly designed telemetric system based on the Internet allows for a remote system control, as shown in an example of the system's operation in Książ (Poland) seismological observatory.

**Key words:** fibre-optic device, seismograph, rotational seismic events.

## 1. INTRODUCTION

A possibility of the existence of rotational motions in the seismic field has been discussed from the beginning of the earthquakes investigations. The interest in this phenomenon has been stimulated by strange, rotary and even screw-like deformations after earthquakes, often appearing on the parts of the tombs and monuments (Kozák 2006, Ferrari 2006). The classical textbooks on seismology deny the possibility that rotational motions, especially in form of seismic rotational waves (SRW) could pass through a rock, so the rotational effects of earthquakes were explained by an interaction of standard seismic waves with a compound structure of the objects they penetrate, which, in fact, might be the case (Teisseyre and Kozák 2003). Nevertheless, it was proved theoretically that even the SRW could propagate through grained rocks; later on, this possibility was extended on rocks with microstructure or defects (Eringen 1999, Teisseyre and Boratyński 2002) or even without any internal structure (Teisseyre 2005, Teisseyre *et al.* 2005, Teisseyre and Górski 2009), due to the asymmetric stresses in the medium. The SRW were for the first time effectively recorded in Poland in 1976 (Droste and Teisseyre 1976). From this time, waves of this type have been studied in a few centers over the world. Recently, the first monographs have been published (Teisseyre *et al.* 2006, Lee *et al.* 2009), covering the theoretical aspects of the rotation motion generation and propagation, as well as the examples of the field experiments.

A further experimental verification of the above research required a new approach to the construction of the measuring devices (Teisseyre *et al.* 2008) because the conventional seismographs are inertial sensors of only linear velocities. For the above reason, the new instrumentations are important, especially those designed for an investigation of very small rotations with the amplitude in the range of  $10^{-9}$  rad/s. Since the Sagnac effect (Sagnac 1913) measures rotation directly, an application of the sensor based on this effect seems to be ideal for the construction of the rotational seismometer. We distinguish two such systems: a ring laser (Schreiber *et al.* 2001), and a fiber-optic (Takeo *et al.* 2002, Jaroszewicz *et al.* 2003), both based on a technical implementation of the Sagnac interferometer for an appropriate detection of very small phase changes generated by this effect. The main advantage of such a system is a possibility to detect the absolute rotation, impossible to be measured in any other way. It seems that the data obtained in this way is easy for an identification.

Based on the experience gained during construction and application of the Fibre-Optic Rotational Seismometer (FORS-II; Jaroszewicz and Krajewski 2008), in this paper we have described our advantageous research leading to a new system named Autonomous Fibre-Optic Seismograph (AFORS). A higher accuracy, compactness as well as a special signal processing unit ensure the autonomous operation of this instrument, which can be monitored as well as

remote-controlled *via* Internet. In the next section, we describe the optical and electronic parts of the AFORS. In Section 3, the system calibration and the noise investigation data are presented. Finally, in Section 4, the first results obtained with the AFORS deployed in the Książ seismological observatory are reported.

## 2. AUTONOMOUS FIBRE-OPTIC SEISMOGRAPH CONSTRUCTION

The optical head of the AFORS system uses a fibre interferometer in the so-called minimum optical gyro configuration (Jaroszewicz *et al.* 2006), as shown in Fig. 1. The optical light from the low-coherence superluminescence diode (SLD) is inserted by the symmetric X-type coupler into two opposite directions of the loop containing a single-mode fibre. The use of the same input and output arm of the coupler assures the reciprocity conditions for two interfering beams in the coupler output but needs an additional coupler to separate a returned beam to a detector as well as a fibre optic isolator for the SLD protection against the returned optical power. The system of two fibre depolarizers (except for SLD and in sensor loop) eliminates an influence of polarization instability from the AFORS operation. The set of cascade polarizers protects the selection of the true single mode input/output operation of the whole system and guarantees that only the nonreciprocal effect in the system provides the Sagnac effect. The last one generates the phase shift equal to (Post 1967)

$$\Delta\phi = \frac{4\pi RL}{\lambda c} \Omega \equiv \frac{1}{S_0} \Omega, \quad (1)$$

where  $R$  is the radius of sensor loop,  $L$  is the length of the optical fibre used in the sensor loop,  $\lambda$  is the wavelength of the light source,  $c$  is the light speed in vacuum,  $\Omega$  is the rotation speed measured in the direction perpendicular to the sensor loop plane.

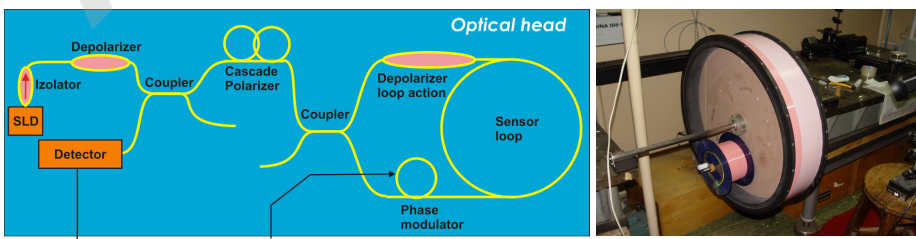


Fig. 1. General schema of the optical head of the AFORS system constructed and the sensor loop winding. Colour version of this figure is available in electronic edition only.

Since we are interested in detecting the extremely small rotation,  $\Omega$ , the method of reducing the so-called optical constant,  $S_0$ , should be used to obtain a high sensitivity of the system. A theoretical system limitation can be determined by an investigation with a minimal rotation speed,  $\Omega_{\min}$ , in the quantum noise limitation according to Ostrzyżek (1989) and is expressed as

$$\frac{\Omega_{\min}}{\sqrt{\Delta B}} = \frac{\lambda c}{4\pi R L} \frac{4\sqrt{2} \times 10^{\alpha/10 \cdot L/1000}}{S J_1(1.84) P_L \times 10^{-\sigma/10}} \times \sqrt{\frac{V_A^2}{R_0^2} + \frac{1}{8} e S P_L \times 10^{-\sigma/10} \times 10^{\alpha/10 \cdot L/1000} (1 + X) + \frac{4kT}{R_0} + I_A^2}, \quad (2)$$

where  $\Delta B$  is detection bandpass,  $\alpha$  is the fibre attenuation in dB/km,  $\sigma$  the total loss in optical part (without loss of the fibre used in sensor loop),  $P_L$  the optical power of the source,  $S$  the sensitivity of the photodiode,  $V_A$  and  $I_A$  are the dark voltage and current of photodiode, respectively;  $R_0$  is the photodiode impedance,  $e$  is the electron charge,  $k$  is the Boltzmann constant, and  $T$  is temperature.

As one can see, some of the above mentioned parameters are difficult to be optimized because they are connected to the optoelectronic element used. However, the system sensitivity can be generally enlarged by increasing the total optical power,  $P_L$ , and the loop radius,  $R$ , whereas the wavelength,  $\lambda$ , the fibre attenuation,  $\alpha$ , as well as the total optical loss of the system,  $\sigma$ , should be minimized. The above comments are also related to the optimal length,  $L$ , of the fibre; its increase generally improves the sensitivity. However, because in a such situation the total length is related to the signal attenuation *via* fibre attenuation,  $\alpha$ , the optimal length is the same as that shown on the simulation presented in Fig. 2.

Taking into consideration the above-mentioned conditions, the developed optical head uses about 15 000 m of a standard SMF-28 fibre (Corning), double-quadropole wound (Dai *et al.* 2002) on a specially constructed composite surface which contains a perlmaloy particles admixture for a sensor loop shelling from the magnetic pool. In general, the temperature influences the constructed sensor performance, and this can create a problem (Jaroszewicz 2001), because the sensor loop has an extreme size of 0.68 m in the diameter and 12.5 cm in height, and contains 15 layers of fibre. For the above reason, a method of the thermally-induced nonreciprocity (Shupe 1980) reduction by the above-mentioned special fibre winding with an additional 0.2 mm Teflon for each layer separation has been applied. Since the temperature conditions in a seismological observatory are generally stable, with the maximum fluctuation around 2-4° per day, the temperature-generated drift of an output signal from the AFORS is compensated enough.

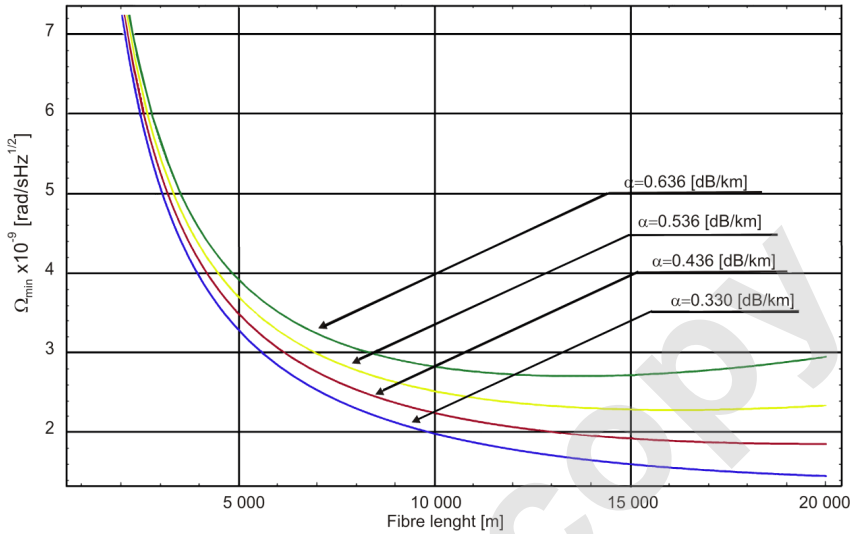


Fig. 2. Simulation of an influence of the fibre length on the AFORS sensitivity. The parameters of Corning SMF-28 fibre as well as Exalos SLD have been used. Colour version of this figure is available in electronic edition only.

However, such a construction of the loop generates an increase in the fibre attenuation from 0.330 dB/km for Corning data to 0.436 dB/km measured after the loop preparation. Moreover, to provide a slow drift in a long period of time, the AFORS uses a cascade of two fibre-optic polarizers (Phoenix Photonics) with a high extinction ratio (46 and 55 dB) and generally operates by applying the depolarized light. For that reason, a set of two fibre depolarizers has been used. One of these (Phoenix Photonics) is placed behind the source and has the extinction ratio equal to 0.02 dB optimized with respect to the source used. As the optical source, the 20.8 mW optical power SLD type 561-HP2-DIL-SM (Exalos) with 31.2 nm bandwidth operating at the central wavelength equal to 1326.9 nm has been used. The second depolarizer is the sensor loop whose performance is equivalent to the depolarizer for the wide-band source used and long SMF-28 fibre, as shown by Krajewski *et al.* (2005) for the simulation of an output degree of polarization from the loop. The additional fibre elements: two couplers (Phoenix Photonics), the isolator (ADC) together with precision splices of all optical elements keep the total optical loss of the AFORS at the level of  $\sigma$  equal to 13.33 dB. Since the InGaAs photodiode (Laser Instruments) with  $I_d = 0.06$  nA,  $S = 0.99$  A/W, and  $R_0 = 163$  k $\Omega$  has been applied, the theoretical sensitivity of the constructed system calculated according to eq. (2) is  $1.97 \times 10^{-9}$  rad/s $^{1/2}$ .

Since the Sagnac phase shift (eq. (1)) obtained directly in an interferometric system contains an unseparated noise component, the special signal processing is used. We have used the system based on the synchronic detection unit (Ostrzyżek 1989). To this end, the phase fibre optic modulator is inserted into the sensor loop near one of the loop ends (Fig. 1). This element of a harmonic power supply generates the additional phase shift described as

$$\phi_m(t) = \phi_0 \sin(\omega_m t), \quad (3)$$

where  $\phi_0$  and  $\omega_m$  are the amplitude and angular frequency of the phase modulation, respectively.

For such an approach, the output intensity from the optical head (before the detector) can be described (Ostrzyżek 1989) as

$$\begin{aligned} I(t) &= P_0 \{1 + \cos[\Delta\phi + \phi_m(t) - \phi_m(t + \tau)]\} \\ &= P_0 \left\{ \begin{aligned} &1 + \cos(\Delta\phi) \left[ J_0(\phi_e) + 2 \sum_{n=1}^{\infty} J_{2n}(\phi_e) \cos(2n\omega_m t') \right] \\ &+ \sin(\Delta\phi) \left[ 2 \sum_{n=1}^{\infty} J_{2n-1}(\phi_e) \sin[(2n-1)\omega_m t'] \right] \end{aligned} \right\}, \quad (4) \end{aligned}$$

where  $t' = t + \tau/2$ ,  $\phi_e = 2\phi_0 \sin(\omega_m \tau/2)$ ,  $2P_0$  is the optical power output,  $\tau$  is the time for light passing throughout a sensor loop.

For a properly chosen angular frequency of the phase modulator which should be correlated with a time delay for the light passing through the sensor loop (for AFORS equal to 6.8 kHz), only first two harmonics of the output signal are important. In such an approach, the Sagnac phase shift can be obtained from the first ( $A_{1\omega}$ ) and the second ( $A_{2\omega}$ ) amplitude of the harmonic output signal as (Krajewski 2005)

$$\Delta\phi = \arctan \left[ \frac{J_2(\phi_e) A_{1\omega}}{J_1(\phi_e) A_{2\omega}} \right] = \arctan [S_e u(t)], \quad u(t) = \frac{A_{1\omega}}{A_{2\omega}}, \quad (5)$$

where  $S_e$  is the electronic constant related to the parameters of the electronics components used.

According to the above, the final relation for the AFORS detected rotation component,  $\Omega$ , can be easily described by two constants, the optical  $S_0$  and electronic  $S_e$ , as

$$\Omega = S_0 \arctan [S_e u(t)]. \quad (6)$$

It should be underlined that the above approach gives the methodology for constructing all electronic units for AFORS; its difficulties are related to the protection of a highly dynamic range during the detection of the first two signal harmonics with the expected high differences of their values. For the above reason, the constructed (see Fig. 3) Autonomous Signal Processing Unit (ASPU; Elproma) contains in the first the special lowpass filters for a proper separa-

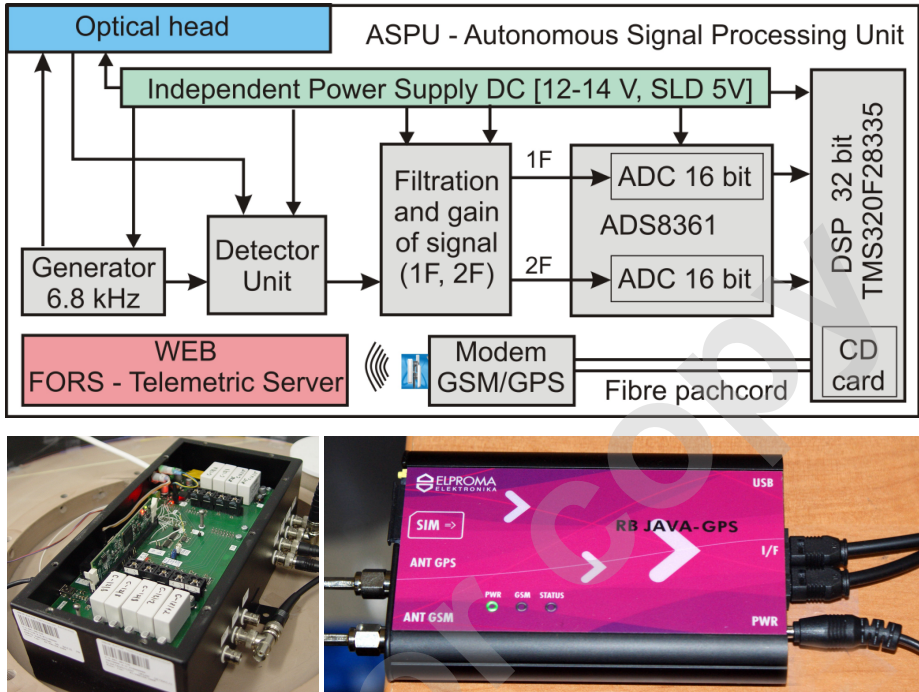


Fig. 3. General scheme and view of the Autonomous Signal Processing Unit of the AFORS. Colour version of this figure is available in electronic edition only.

tion and the gain of the first and second harmonics from a signal detected by the photodiode. The next such separated components are converted into digital signals by the ADS8361 containing two 16 bit ADC modules from which amplitudes  $A_{1\omega}$  and  $A_{2\omega}$  in digital forms are processed by the Digital Signal Processing (DSP) module according to the authors' procedure based on eqs. (3) and (4) for determining the value of rotation rate,  $\Omega$ . The 32-bit signal processor TMS320F28335 (Texas Instruments) working with a frequency of 150 MHz has been used as an optimal DSP unit, because it enables calculation on the basis of signal frames having 1024 length of 16-bit samples. Finally, the obtained results are stored on a CD card and transmitted by a GSM/GPS module to a special WEB FORS – Telemetric Server. The FORS – Telemetric Server is used for the data storage, the monitoring the AFORS work, as well as for the remote control of their parameters. Since the ASPU contains an additional independent power supply for all electronic components of the system, the AFORS is a fully autonomous and mobile system for investigating the rotational components existing during seismic events.

### 3. AFORS CALIBRATION AND THE ESTIMATION OF ACCURACY

Since the AFORS operation is based on properly defined values of the two constants, optical  $S_0$  and electronic  $S_e$  (see eq. (6)), which are impossible to be determined in an analytical way with a required precision, a special calibration process has been used for their determination. The method used was based on the measurement of a well defined slow rotation connected to the vector component of the Earth rotation in Warsaw (*i.e.*,  $\Omega_E = 9.18 \text{ deg/h} \equiv 4.45 \times 10^{-5} \text{ rad/s}$  for  $\phi = 52^\circ 20''$ ) on a special system positioning as shown in Fig. 4 (Jaroszewicz *et al.* 2001). The AFORS is mounted vertically on a rotation table, and rotates in such way that the sensor loop is directed to the N, E, S, and W. For the directions E-W, the measured rotation is zero because in these directions the plane of the sensor loop is collinear with the Earth rotation axis, whereas for the directions N-S the maximum values of the measured signal are positive or negative, because the sensor loop plane is perpendicular to the vector component of the Earth rotation,  $\Omega_E$ .

Initially, the output parameters of ASPU are undefined, so we used 7280 DSP lock-in amplifier (Perkin Elmer) in the calibration process. From eq. (5), the in system-detected signal  $u(t)$  can be expressed as

$$u(t) = \frac{A_{1\omega}}{A_{2\omega}} = \frac{J_1(\phi_e)}{J_2(\phi_e)} \tan \Delta\phi \tag{7}$$

hence

$$S_e = \frac{A_{2\omega}}{A_{1\omega}} \tan \Delta\phi .$$

Therefore, as the first step for the AFORS positioned in N-S directions we read amplitudes  $A_{1\omega}$  and  $A_{2\omega}$  from the lock-in (further on denoted  $LA_{1\omega}$ ,  $LA_{2\omega}$ )

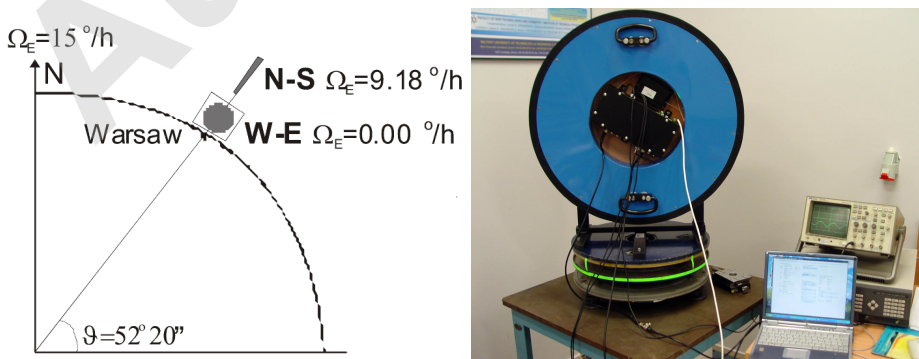


Fig. 4. The scheme showing an idea and general view of AFORS during the calibration process. Colour version of this figure is available in electronic edition only.

and from the ASPU (denoted  $EA_{1\omega}$ ,  $EA_{2\omega}$ ), a comparison of which gives us the information about the electronic constant,  $S_e$ :

$$S_e = \left( \frac{LA_{1\omega}}{LA_{2\omega}} \frac{EA_{2\omega}}{EA_{1\omega}} \right) Z_w, \quad Z_w = \frac{J_2(\phi_e)}{J_1(\phi_e)}, \quad (8)$$

where values in parentheses give the electronic recalibrate of the ASPU indications on the basis of the lock-in indications.

As one can see, what really matters in the calibration procedure is the determination of the real value of  $\phi_e$ . Since from eq. (4) we have

$$A_{2\omega} = 2P_0 J_2(\phi_e) \cos(\Delta\phi), \quad (9)$$

thus, as the second step we measure the value of  $A_{2\omega}$  for a zero value of the Sagnac phase shift  $\Delta\phi$  (AFORS directed W-E) and measure the value of  $2P_0$  (the constant value on oscilloscope equals 3353 mV for AFORS, see Fig. 4) for the system with a switched off modulation from the generator and determine the value of  $J_2(\phi_e)$  as

$$J_2(\phi_e) = \frac{\sqrt{2}A_{2\omega}}{2P_0}. \quad (10)$$

The constant  $\sqrt{2}$  results from the measurement by the lock-in RMS value. Since in the described measurement we have  $J_2(\phi_e) = 0.264917$ , thus  $\phi_e$  has been calculated as 1.63199. On this basis, for recalibrating ASPU indications ( $LA_{1\omega} = 8.2$  mV,  $EA_{1\omega} = 4066$ ,  $LA_{2\omega} = 606.6$  mV,  $EA_{2\omega} = 9390$ ), eq. (8) gives value for electronic constant,  $S_e$ , equal to 0.0144.

Finally for the determined value of  $S_e$  and the recalibrated values of harmonic components of the signal from ASPU ( $EA_{1\omega}$  and  $EA_{2\omega}$ , as  $A_{1\omega}$  and  $A_{2\omega}$ , respectively), the Earth rotation component measurement for AFORS directed in N and S (see Fig. 5) based on eq. (6) gives us the  $S_0$  value equal to 0.00433.

After the proper calibration of the system, the estimation of the AFORS accuracy is the final work. However, this work performed in the MUT laboratory located in Warsaw, Poland, can give only limited information about the system accuracy, which is related to the existence of town noises. This calculation is made for zero value of the Sagnac phase shift  $\Delta\phi$  (AFORS directed in W-E) and the measurement of the level of noises for amplitudes  $A_{1\omega}$  and  $A_{2\omega}$  (their mean values for the switched off modulation from the generator – see Fig. 6). Because eq. (6) can be expressed as

$$\Omega(A_{1\omega}, A_{2\omega}) = S_0 \arctan \left( S_e \frac{A_{1\omega}}{A_{2\omega}} \right), \quad (11)$$

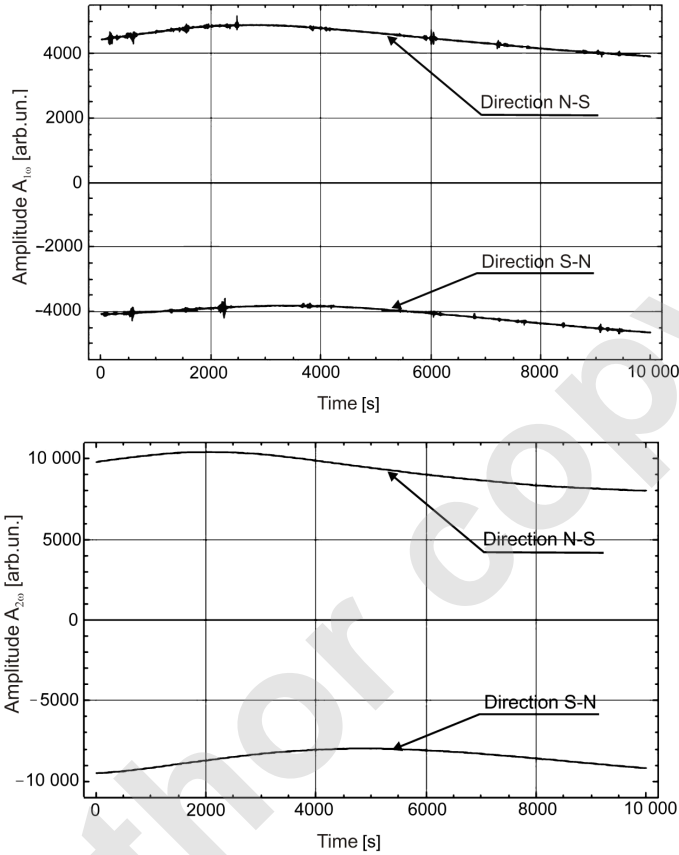


Fig. 5. The amplitudes  $A_{1\omega}$  and  $A_{2\omega}$  of signals from AFORS positioned in N and S directions. The resolution in the S-N and N-S directions is obtained on the basis of the signal phase analysis.

the accuracy  $\Delta\Omega$  of the rotation measured by AFORS for a given measurement bandpass  $\Delta B$  can be found as

$$\Delta\Omega \equiv \sqrt{\left(\frac{\partial\Omega}{\partial A_{1\omega}}\bar{\sigma}_{1\omega}\right)^2 + \left(\frac{\partial\Omega}{\partial A_{2\omega}}\bar{\sigma}_{2\omega}\right)^2}, \quad (12)$$

where  $\bar{\sigma}_{1\omega}$  and  $\bar{\sigma}_{2\omega}$  are mean values of noises recorded for the amplitudes  $A_{1\omega}$  and  $A_{2\omega}$ , as shown in Fig. 6.

Because the construction of the ASPU enables step changes of  $\Delta B$  in the range from 1.66 to 212.30 Hz, the above procedure gives the accuracy from  $5.1 \times 10^{-9}$  to  $5.5 \times 10^{-8}$  rad/s, which is well correlated with the minimal rotation speed,  $\Omega_{\min}$ , in quantum noise limitation, as shown in Fig. 7.

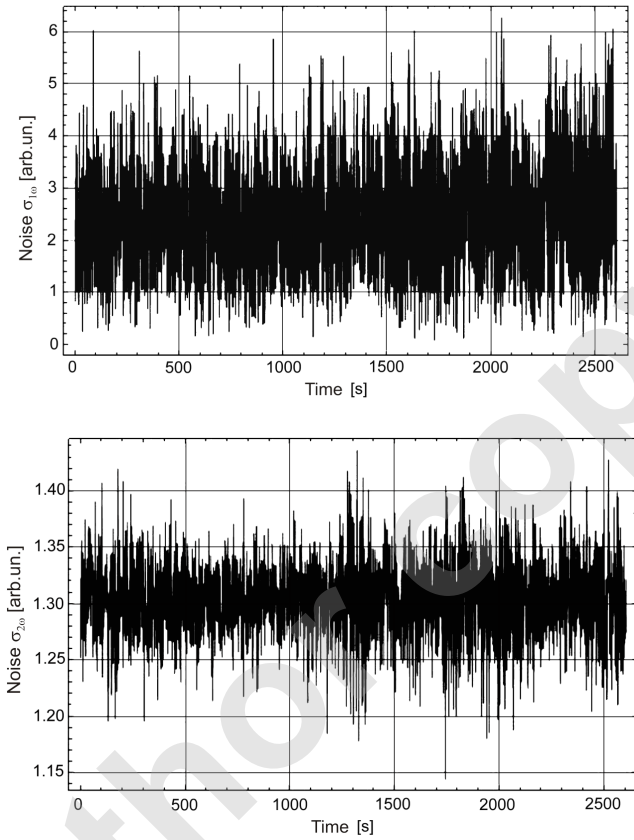


Fig. 6. The noise of signal components  $A_{1\omega}$  and  $A_{2\omega}$  in the 20 Hz detection bandpass.

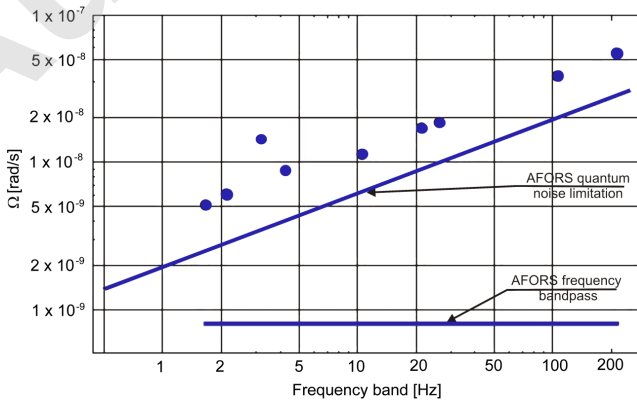


Fig. 7. The AFORS accuracy measured for the chosen detection bandpass.

It should be noted that the linear dependence of the AFORS sensitivity and accuracy with respect to the detection bandpass is the challenge of this system according to the expected frequency characteristics of rotational seismic waves (Teisseyre *et al.* 2006).

#### 4. RESULTS OF SEISMIC ROTATION COMPONENTS RECORDING IN THE KSIĄŻ SEISMOLOGICAL OBSERVATORY

The system AFORS-1 has been installed in the Książ seismological observatory in Poland since July 2010 with its continuous monitoring through the Internet basing on the application “FORS Telemetric Server”, as shown in Fig. 8, which can manage the set of FORS.

The server ensures the full remote control for each FORS manufactured in the AFORS technology. In this paper we describe the AFORS system installed in the Książ observatory labelled at the server as AFORS-1, AFORS-2 identical with previous ones (under investigation in MUT laboratory), SIM-FORS-II virtual system located in Elpoma (used for testing a new software for ASPU), and AFORS-3 (during the R&D reconstruction of an electronic part for AFORS technology on the FORS-II system installed in Ojców Observatory, Poland; see Jaroszewicz and Krajewski 2008) as it is shown in Fig. 9a for the main bookmark in the catalogue DEVICE. The applied technology gives possibility of a remote (*via* Internet) controlling and changing all the electronic parameters (including software upgrade) of the ASPU for a given AFORS as presents in the bookmark CONFIG for the AFORS-1 in Fig. 9b. Moreover, the next bookmark, DATA&VARIABLES (see Fig. 9c), enables monitoring in a real time of the main data and variables for AFORS with a possibility of a remote changing of the level of signals which initialize the automatic data stored on a CD card and its transfer *via* GSM. Finally, the bookmark GSM/GPS (Fig. 9d) is for monitoring in real time the GSM parameters as well as the GPS parameters which include the AFORS global localization which could be visualized by the Google map *via* the button “Mapa”. Additionally, for an operator’s comfort, the top right corner of the bookmarks for a given system located in server contains information about a current date and time and the four main parts of AFORS state of work (good as green, partial good as yellow or no work as black color), *i.e.*, FORS – recording power in system, GSM – detection by system GSM signal, COM – existing communication between AFORS and server, and GPS – GPS signal detection by the system GPS. In this way, it is possible to monitor any seismograph made in the AFORS technology from any place with the access to Internet, which is an innovative solution.

Other bookmarks named Measurement (see Fig. 8b or 9a) collected the data recorded by the devices existing in the server. Figure 10 shows for example two

(a)



(b)

MILITARY UNIVERSITY OF TECHNOLOGY  
Institute of Applied Physics

## FORS – Telemetric Server

- Start
- Measurements
- Devices
- Albums
- Users
- Organizations
- Logout

**FORS-TS**  
Fiber-Optic Rotational Seismographs Telemetric System v.10.7 developed for remote control and data collection from installed FORSS in seismological laboratories.

**Authors**  
Leszek R. Jaroszewicz  
PhD (DSc) (Eng)  
Henryk A. Kowalski  
MSc (Eng)  
Jerzy K. Kowalski  
PhD (Eng)  
Zbigniew Krajewski  
PhD (Eng)  
Grzegorz Mazur  
MSc (Eng)  
Paweł Zimowski  
MSc (Eng)

The logo of the Military University of Technology (WAT) is a stylized double-headed eagle with a crown on its head, set within a shield-like border. The letters 'WAT' are prominently displayed at the bottom of the shield.

Fig. 8: (a) The general view of AFORS-1 installed in Książ observatory, as well as (b) main page of FORS Telemetric Server located at <http://fors.m2s.pl>. Colour version of this figure is available in electronic edition only.

such data obtained from AFORS-1. This data shows the proper work of AFROS as a system for rotational motion detection, and they are very promising for the future investigation in Książ by an application of the system described here.

(a)

**MILITARY UNIVERSITY OF TECHNOLOGY**  
Institute of Applied Physics

- Start
- Measurements
- Devices
- Albums
- Users
- Organizations
- Logout

**FORS-TS**  
Fiber-Optic Rotational Seismographs  
Telemetric System v.10.7 developed for remote control and data collection from installed FORSs in seismological laboratories.

**Authors**  
Leszek R. Jaroszewicz  
PhD (Sc Eng)  
Henryk A. Kowalski  
MSc (Eng)  
Jerzy K. Kowalski  
PhD (Eng)  
Zbigniew Krajewski  
PhD (Eng)  
Grzegorz Mazur  
MSc (Eng)  
Paweł Zińwoko  
MSc (Eng)

## FORS – Telemetric Server

2011-01-24

**Devices** New

Search:  Name:  Address:  City:  Contact:

C S >

Find: 4

ID #	IMEI	Name	Address	City	Contact	FORS	GPS	COMM	GSM		
1	000000123456789	SIM FORS-II	ELPROMA	Łomianki	Paweł Zińwoko	-	-	-	-	L	E
2	355833010028533	AFORS-1	Książ Castel	Książ	Leszek R. Jaroszewicz	0	0	0	0	L	E
8	355832010131776	AFORS-2	Kaliskiego 2	MUT Warsaw	Leszek R. Jaroszewicz	0	0	1	0	L	E
9	355832010107644	AFORS-3 (R&D)	Kaliskiego 2	MUT Warsaw	Paweł Zińwoko	-	-	-	-	L	E

© m-Soft Sp. z o.o. 2008-2011 Created by m-Soft

(b)

Config

Data&Variables

GSM/GPS

2011-01-24 20:32:53 FORS GPS COMM GSM

**AFORS ID: 2 IMEI: 355833010028533 (last read: 2011-01-24 19:03:32)**

**Manual Configuration**

**PGA Amplification**

S1 (A): 8.9125089645386x [230] (0.255) 19dB

S2 (B): 1.5848932266235x [200] (0.255) 4dB

**Sinus Voltage**

Sin A: 220 (0.655 mV)

Sin B: 220 (0.655 mV)

**Amplification BRF** vb

BRF1: 32000

BRF2: 32000

**DAC Coefficients**

deg: 100000

rad: 100000

**k for Omega**

K1: 4.1000000E-3

K2: 5.5999998E-3

**Measurement time constant**

t: 10 x 4.7104 ms

**Auto Configuration**

Omega Auto-offset: undefined

INC OM:

**XY Auto-Zero Corection**

Calculate & Turn On  Reset Value  NC

**Auto Gain&Phase**

Auto Gain  Auto Phase

**Current Configuration**

Load  Write  Refresh  NC

Set Time

**Parameters**

**Analog Outputs: ---**

5

**Laser Settings**

ON  OFF  NC  RST

**Increase and decrease F parameter**

+  -  NC

**SMS numbers**

SMS #1: undefined

SMS #2: undefined

SMS #3: undefined

**E-Mail**

E-mail #1: undefined

E-mail #2: undefined

E-mail #3: undefined

**DSP firmware:**

Load  Program

Act. ver: DigiFors\_v2.048

**Upload firmware** [Cancel](#)

File name	Upload time	Size
DigiFors2048.hex	2010-09-17 11:24:04	153kB

C
Set parameters

Figure continued on next page.

(c)

Config
Data&Variables
GSM/GPS

2011-01-24 20:35:14
FORS
GPS
COMM
GSM

**Data download & trigger level**

RDF FS:  L:

RD Last sec.:

GF

Level	Before [block]	After [block]
<input type="checkbox"/> GS		
Level [ADEV]	Buf Len[sps]	
Before[block]	After[block]	

<b>Omega Average Deviation:</b>	5.1915517E-8	rad/s
<b>Omega:</b>	-4.097069279E-7	rad/s
<b>GF Level:</b>	3034240041	
<b>GF Before:</b>	10	block
<b>GF After:</b>	10	block
<b>GS Level:</b>	16	ADEV
<b>GS Buf Len:</b>	64	sps
<b>GS Before:</b>	10	block
<b>GS After:</b>	10	block
<b>GS T:</b>	0001	
<b>GS TM:</b>	0000	

C Refresh
Set

**Variables Values [2011-01-24 20:34:10]**

Omega in rad/s:	-4.097069279E-7
Omega Offset in rad/s:	6.178327749E-5
Omega offset flag:	0014
R1mean:	14417.520507812
R2mean:	7931.2416992188
Max A/B:	18746 / 15337
XY Auto-Zero set flag:	0000
LIA auto phase set flag:	0
uin:	13.476438522339
F1:	6799.9497070312
F2:	13599.899414062
F0:	217598.390625

(d)

Config
Data&Variables
GSM/GPS

2011-01-24 20:35:53
FORS
GPS
COMM
GSM

**GSM: 2011-01-24 20:34:12**

hconf:	G24 OEM Module
imei:	355833010028533
gprsreg:	Registered 2:1
gsmreg:	;1:1
opalpha:	Era
opnum:	260-2
covstat:	GPRS coverage 1
signalber:	99 brutto 111.57 PLN,
signalrssi:	20 20
cellid:	49535
celllac:	42220
wersja:	2010122810
komendy:	Y1;C1;C2;C3;K1;Y1;
dane:	init
diff:	4338
pobieranie:	false
time:	1295894024063
Czas Long:	Mon Jan 24 19:33:53 GMT+01:00 2011
Czas RTC:	193353GMT+01:00
Data RTC:	240111truefalse
Phone1:	Mon Jan 24 19:33:53 GMT+01:00 20111295894033359
Phone2:	Mon Jan 24 19:33:53 GMT+01:00 20111295894033376

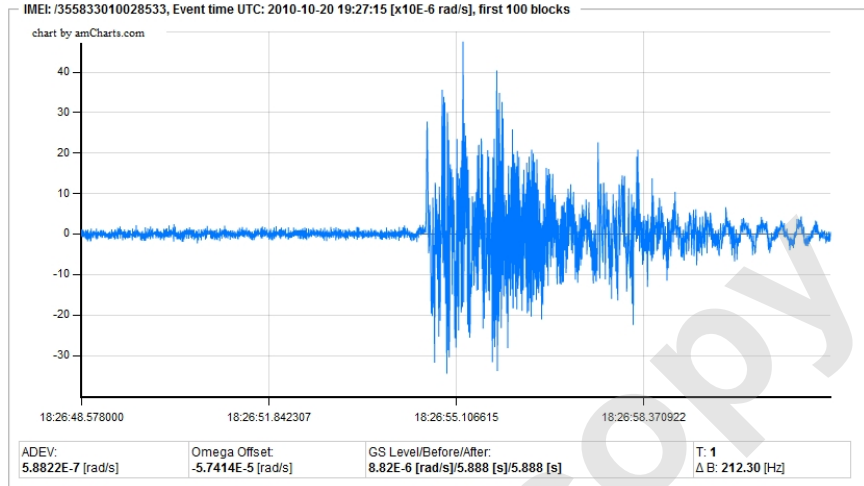
**GPS: 2011-01-24 20:35:23**

imei:	355833010028533
lati:	5050.5964
latins:	N
long:	01617.5194
longwe:	E
fix:	1
nrofsat:	07
alti:	358.0
time:	193520.000
date:	240111
lati_g:	50.84327333
long_g:	16.29199

Mapa

Fig. 9. The view of four main bookmarks for AFORS-1 at FORS Telemetric Server. Colour version of this figure is available in electronic edition only.

## Measurements



## Measurements

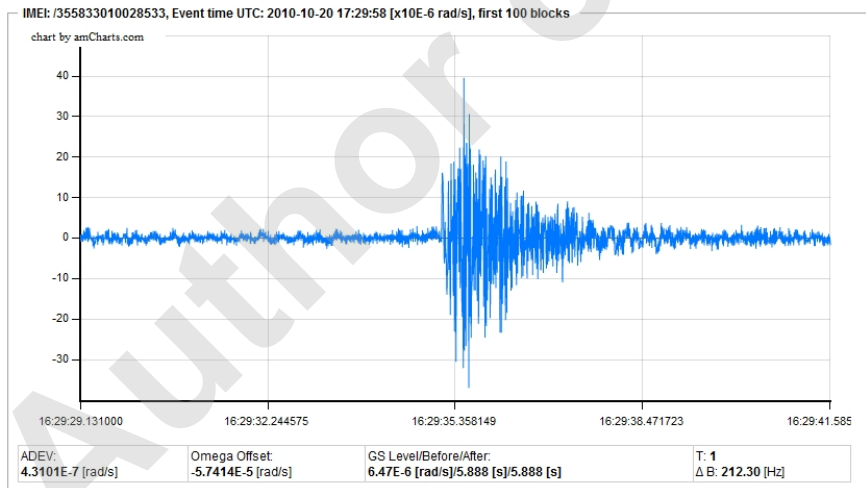


Fig. 10. The seismograms recorded by AFORS-1 in Książ on 20 October 2010. The amplitude of the recorded data is identified in the middle part of the top line; at the bottom, we show the main parameters of AFORS in the recording time: ADEV – Omega Average Deviation, Omega Offset, GS Level/Before/After – adjusted level of signal for data stored, and  $\Delta B$  – adjusted detection bandpass.

## 5. CONCLUSIONS

The presented instrument AFORS-1 with the accuracy in the range between  $5.1 \times 10^{-9}$  and  $5.5 \times 10^{-8}$  rad/s, depending on the detection bandpass which

is in the range of 1.66 to 212.30 Hz, seems to be an attractive device for the investigation of rotational components existing in seismic events. The main advantage of this system is its high accuracy with linear changes in the whole detection bandpass. Such a characteristic is not attainable for any seismological device based on the inertia systems. Since the AFORS operation is based on the detection of Sagnac effect, the AFORS is insensitive to linear motions and accelerations, and it detects the absolute rotation in a real time, which is also impossible to be realized in any other way. The Internet application for a system monitoring, data storage and their remote control, simplifies the device maintenance and protects the full remote control of the system. The first result obtained in the Książ Observatory gives hope for the future exploitation of the system.

**A c k n o w l e d g e m e n t s.** This work was done in the years 2009-2010 under the financial support from the Polish Ministry of Science and Higher Education under contract No. 2166/B/T02/2007/33 and partially (software for server) Key Project POIG.01.03.01-14-016/08 "New photonic materials and their advanced application".

## References

- Dai, X., X. Zhao, B. Cai, G. Yang, K. Zhou, and C. Liu (2002), Quantitative analysis of the Shupe reduction in a fiber-optic Sagnac interferometer, *Opt. Eng.* **41**, 6, 1155-1156, DOI: 10.1117/1.1478078.
- Droste, Z., and R. Teisseyre (1976), Rotational and displacemental components of ground motion as deduced from data of the azimuth system of seismographs, *Publs. Inst. Geophys. Pol. Acad. Sc.* **M-1**, 97, 157-167.
- Eringen, A.C. (1999), *Microcontinuum Field Theories. Vol. 1. Foundations and Solids*, Springer Verlag, New York
- Ferrari, G. (2006), Note on the historical rotation seismographs. **In:** R. Teisseyre, M. Takeo, and E. Majewski (eds.), *Earthquake Source Asymmetry, Structural Media and Rotation Effects*, Springer, Berlin, 367-376.
- Jaroszewicz, L.R. (2001), Polarisation behaviour of different fiber-optic interferometer configurations under temperature changes, *Opt. Appl.* **31**, 399-423.
- Jaroszewicz, L.R., and Z. Krajewski (2008), Application of fibre-optic rotational seismometer in investigation of seismic rotational waves, *Opto-Electron. Rev.* **16**, 3, 314-320, DOI: 10.2478/s11772-008-0015-2.

- Jaroszewicz, L.R., Z. Krajewski, and R. Świłło (2001), Application of fiber-optic Sagnac interferometer for detection of rotational seismic events, *Mol. Quan. Acoust.* **22**, 133-144.
- Jaroszewicz, L.R., Z. Krajewski, L. Solarz, P. Marć, and T. Kostrzyński (2003), A new area of the fiber-Sagnac interferometer application, *International Microwave and Optoelectronics Conference (IMOC 2003): Proc. 2003 SBMO/IEEE MTT-S, 20-23 Sept., Iguazu Falls, Brazil*, Vol. 2, IEE, Piscataway, NJ, 661-666, DOI: 10.1109/IMOC.2003.1242657.
- Jaroszewicz, L.R., Z. Krajewski, L. Solarz, and R. Teisseyre (2006), Application of the fibre-optic Sagnac interferometer in the investigation of seismic rotational waves, *Meas. Sci. Technol.* **17**, 5, 1186-1193, DOI: 10.1088/0957-0233/17/5/S42.
- Kozák, J.T. (2006), Development of earthquake rotational effect study. **In:** R. Teisseyre, M. Takeo, and E. Majewski (eds.), *Earthquake Source Asymmetry, Structural Media and Rotation Effects*, Springer, Berlin, 3-10.
- Krajewski, Z. (2005), Fiber optic Sagnac interferometer as device for rotational effect investigation connected with seismic events, Ph.D. Thesis, Military University of Technology (in Polish).
- Krajewski, Z., L.R. Jaroszewicz, and L. Solarz (2005), Optimization of fiber-optic Sagnac interferometer for detection of rotational seismic events, *Proc. SPIE* **5952**, 240-248, DOI: 10.1117/12.620620.
- Lee, W.H.K., M. Çelebi, M.I. Todorovska, and H. Igel (2009), Introduction to the Special Issue on rotational seismology and engineering applications, *BSSA* **99**, 2B, 945-957, DOI: 10.1785/0120080344.
- Ostrzyżek, A. (1989), Accuracy analyze of angle speed measurement in the fiber optic gyroscope, Ph.D. Thesis, Military University of Technology (in Polish).
- Post, E.J. (1967), Sagnac effect, *Rev. Mod. Phys.* **39**, 2, 475-493, DOI: 10.1103/RevModPhys.39.475.
- Sagnac, G. (1913), L'éther lumineux démontré par l'effet du vent relatif d'éther dans un interféromètre en rotation uniforme, *Comptes-rendus de l'Académie des Sciences* **95**, 708-710 (in French).
- Schreiber, U., M. Schneider, C.H. Rowe, G.E. Stedman, and W. Schlüter (2001), Aspects of ring lasers as local Earth rotation sensors, *Surv. Geophys.* **22**, 5-6, 603-611, DOI: 10.1023/A:1015640822274.
- Shupe, D.M. (1980), Thermally induced nonreciprocity in the fiber-optic interferometer, *Appl. Opt.* **19**, 5, 654-655, DOI: 10.1364/AO.19.000654.
- Takeo, M., H. Ueda, and T. Matzuzawa (2002), Development of high-gain rotational-motion seismograph, Grant 11354004, Earthquake Research Institute, Univ. of Tokyo, 5-29.
- Teisseyre, R. (2005), Asymmetric continuum mechanics: deviations from elasticity and symmetry, *Acta Geophys.* **53**, 2, 115-126.
- Teisseyre, R., and W. Boratyński (2002), Continuum with self-rotation nuclei: Evolution of defect fields and equations of motion, *Acta Geophys.* **50**, 2, 223-229.
- Teisseyre, R., and M. Górski (2009) Transport in fracture processes: fragmentation

- and slip, *Acta Geophys.* **57**, 3, 583-599, DOI: 10.2478/s11600-009-0020-y.
- Teisseyre, R., and J.T. Kozák (2003), Considerations on the seismic rotation effects, *Acta Geophys.* **51**, 3, 243-256.
- Teisseyre, R., M. Białecki, and M. Górski (2005), Degenerated mechanics in a homogeneous continuum: potentials for spin and twist, *Acta Geophys.* **53**, 3, 219-230.
- Teisseyre, R., M. Takeo, and E. Majewski (2006), *Earthquake Source Asymmetry, Structural Media and Rotation Effects*, Springer, Berlin
- Teisseyre, R., H. Nagahama, and E. Majewski (2008), *Physics of Asymmetric Continuum: Extreme and Fracture Processes. Earthquake Rotation and Soliton Waves*, Springer-Verlag, Berlin-Heidelberg

Received 19 August 2010

Received in revised form 5 January 2011

Accepted 19 January 2011